


High-resolution multi- T_1 -weighted contrast and T_1 mapping with low B_1^+ sensitivity using the fluid and white matter suppression (FLAWS) sequence at 7T

Jérémy Beaumont^{1,2}  | Giulio Gambarota¹ | Hervé Saint-Jalmes¹ | Oscar Acosta¹ | Jean-Christophe Ferré^{3,4} | Parnesh Raniga² | Jurgen Fripp²

¹Univ Rennes, CRLCC Eugene Marquis, Inserm, LTSI-UMR1099, Rennes, France

²The Australian e-Health Research Centre, CSIRO, Brisbane, Australia

³Univ Rennes, Inria, CNRS, Inserm, IRISA, EMPENN ERL U-1228, Rennes, France

⁴CHU Rennes, Department of Neuroradiology, Rennes, France

Correspondence

Jérémy Beaumont, Univ Rennes, CRLCC Eugene Marquis, Inserm, LTSI-UMR1099, F-35000 Rennes, France.
Email: jeremy.beaumont.2@gmail.com

Funding information

“Region Bretagne” (France)

Purpose: To demonstrate that fluid and white matter suppression (FLAWS) imaging can be used for high-resolution T_1 mapping with low transmitted bias field (B_1^+) sensitivity at 7T.

Methods: The FLAWS sequence was optimized for 0.8-mm isotropic resolution imaging. The theoretical accuracy and precision of the FLAWS T_1 mapping was compared with the one of the magnetization-prepared two rapid gradient echoes (MP2RAGE) sequence optimized for low B_1^+ sensitivity. FLAWS images were acquired at 7T on six healthy volunteers (21 to 48 years old; two women). MP2RAGE and saturation-prepared with two rapid gradient echoes (SA2RAGE) datasets were also acquired to obtain T_1 mapping references and B_1^+ maps. The contrast-to-noise ratio (CNR) between brain tissues was measured in the FLAWS-hco and MP2RAGE-uni images. The Pearson correlation was measured between the MP2RAGE and FLAWS T_1 maps. The effect of B_1^+ on FLAWS T_1 mapping was assessed using the Pearson correlation.

Results: The FLAWS-hco images were characterized by a higher brain tissue CNR ($CNR_{WM/GM} = 5.5$, $CNR_{WM/CSF} = 14.7$, $CNR_{GM/CSF} = 10.3$) than the MP2RAGE-uni images ($CNR_{WM/GM} = 4.9$, $CNR_{WM/CSF} = 6.6$, $CNR_{GM/CSF} = 3.7$). The theoretical accuracy and precision of the FLAWS T_1 mapping (acc = 91.9%; prec = 90.2%) were in agreement with those provided by the MP2RAGE T_1 mapping (acc = 90.0%; prec = 86.8%). A good agreement was found between in vivo T_1 values measured with the MP2RAGE and FLAWS sequences ($r = 0.91$). A weak correlation was found between the FLAWS T_1 map and the B_1^+ map within cortical gray matter and white matter segmentations ($r_{WM} = -0.026$; $r_{GM} = 0.081$).

Conclusion: The results from this study suggest that FLAWS is a good candidate for high-resolution T_1 -weighted imaging and T_1 mapping at the field strength of 7T.

KEYWORDSBrain, FLAWS, MP2RAGE, MRI, T₁ mapping

1 | INTRODUCTION

The increased signal available from 7T MRI has significant clinical potential for the study of human brain structures, enabling improvements in resolution and/or signal-to-noise ratio (SNR) of the acquired data.¹ However, 7T MRI is characterized by an increase in the transmitted (B_1^+) and received (B_1^-) bias fields, which affect image quality and interpretation. To help address this limitation, the magnetization-prepared two rapid gradient echoes (MP2RAGE) sequence was developed to reduce the B_1 sensitivity of T₁-weighted images.² This sequence is designed to acquire two gradient echo images that are coregistered and combined to provide a T₁-weighted image, named MP2RAGE-uni, that is free of T₂^{*} relaxation, proton density (M_0) and B_1^- . In addition, T₁ maps can be generated using lookup tables of the MP2RAGE-uni signal, enhancing the utility of the MP2RAGE sequence compared with the MPRAGE sequence for longitudinal and multicenter studies.³⁻⁵

Marques et al showed that the MP2RAGE-uni signal can be highly B_1^+ dependent according to the parameters used to acquire the gradient echo images.^{2,6} Thus, the reproducibility of the T₁ mapping and cortical thickness measurements can be hampered by the increased transmitted bias field typical from 7T imaging.^{6,7} To overcome this limitation, Marques et al proposed a set of parameters to reduce the B_1^+ sensitivity of the 7T MP2RAGE sequence, at the cost of limiting its resolution and contrast-to-noise ratio (CNR).⁶ In addition, MP2RAGE scans can be post hoc B_1^+ corrected to increase the reliability of T₁ and cortical thickness measurements.^{6,7}

The two three-dimensional (3D) datasets acquired in MP2RAGE have limited clinical utility.² Consequently, Tanner et al proposed a new MP2RAGE optimization scheme, called fluid and white matter suppression (FLAWS), which was designed to acquire two coregistered 3D datasets with clinical relevance.⁸ The FLAWS sequence provides (1) a white matter- (WM-) suppressed contrast in the first 3D dataset, and (2) a cerebrospinal fluid- (CSF-) suppressed contrast in the second 3D dataset, which we will refer to as FLAWS1 and FLAWS2, respectively. In terms of clinical utility, the FLAWS1 contrast facilitates the visualization of deep gray matter (GM) structures.^{8,9} FLAWS2 provides a standard T₁-weighted anatomical contrast.¹⁰ In addition, a GM-specific contrast can be obtained by computing the voxel-wise minimum between FLAWS1 and FLAWS2. This GM-specific contrast is similar in purpose to the T₂-weighted double-inversion recovery contrast,¹¹ which is used to detect WM and intracortical lesions in multiple sclerosis.¹² These

FLAWS properties suggest that this sequence has potential for the detection and segmentation of brain lesions.^{8,13,14} The FLAWS sequence has also been shown to be of interest to visualize basal ganglia structures^{15,16} and to perform brain tissue segmentation.¹⁷

Despite the potential clinical interest provided by the FLAWS sequence, its use has been limited for 7T imaging as it could not provide a bias-reduced T₁-weighted image and its associated T₁ map. Recent studies at 1.5T have proposed a new combination image, named FLAWS-hc (high-contrast FLAWS), to obtain a bias-reduced T₁-weighted contrast with the FLAWS sequence.^{9,18} However, the possibility of measuring the T₁ relaxation time with FLAWS-hc has not been investigated.

In this context, the current study aimed at (1) optimizing the FLAWS sequence for 0.8-mm isotropic resolution 7T acquisition with a FLAWS-dedicated optimization method previously used at 1.5T,⁹ (2) assessing if the FLAWS-hc combination image provides a T₁-weighted contrast with reduced B_1 sensitivity at 7T, and (3) showing that the FLAWS sequence can be used to generate high-resolution T₁ maps with low B_1^+ sensitivity at 7T.

2 | METHODS

2.1 | FLAWS sequence optimization

The FLAWS sequence was optimized at the field strength of 7T using an optimization method previously used for FLAWS at 1.5T imaging.⁹ This optimization method was designed to provide high CNR images with a suppression of the WM (respectively CSF) signal in FLAWS1 (respectively FLAWS2), while ensuring that the signal of the basal ganglia structures, particularly the globus pallidus, is not suppressed in FLAWS1. In accordance with previous FLAWS studies,^{8,9} the globus pallidus was used as a structure of reference in the current study to ensure that the WM signal suppression does not hamper the visualization of deep GM structures in FLAWS1, as FLAWS imaging intends to provide a good visualization of deep GM structures for deep brain stimulation (DBS) surgery planning.^{8,15}

The optimization was performed in two steps: (1) a profit function was maximized under constraints to select multiple preoptimal parameter sets characterized by a high brain tissue signal in FLAWS images, except for the signals of WM in FLAWS1 and CSF in FLAWS2, which were minimized; and (2) the optimal set of parameters was extracted from

the preoptimal parameter sets by maximizing the sum of FLAWS1 and FLAWS2 brain tissue contrasts.

FLAWS1 and FLAWS2 signals were simulated by solving the Bloch equations of the MP2RAGE sequence. Simulations were performed using the Mathematica software (Wolfram Research, Champaign, IL). The following T_1 relaxation times were used to simulate FLAWS signals: 1050 ms for WM, 1347 ms for the globus pallidus, 1850 ms for GM, and 4000 ms for CSF.^{2,19} The proton densities of WM, the globus pallidus, GM, and CSF were assumed to value 0.7, 0.72, 0.8, and 1.0, respectively.

The optimization was designed to allow FLAWS images to be acquired with 0.8-mm isotropic resolution within 10 minutes. To avoid aliasing artifacts and to reduce the acquisition time, images were acquired in the sagittal direction with a matrix size of 300×300 and 192 slices. A slice partial Fourier of 6/8 was used to shorten the minimum first inversion time, thus, allowing to suppress the WM signal in FLAWS1.⁸ Increasing the sequence repetition time allows to increase the signal-to-noise ratio (SNR) of FLAWS images.^{8,9} Therefore, the sequence repetition time was set to 5 seconds to maximize the SNR, while ensuring an acquisition time of 10 minutes according to the resolution constraints. Parallel imaging was used to speed-up the acquisition ($3 \times$ generalized auto-calibrating partially parallel acquisitions [GRAPPA] acceleration).

The optimization was performed with a brute-force search to maximize the profit function and select the optimal parameter set. Sets were defined for a wide range of parameter combinations, with α_1 and α_2 , the flip angles of the sequence, ranging from 3° to 13° (step-size 1°); TI_1 , the first inversion time, ranging from 0.26 seconds to 1.80 seconds (step-size 0.02 seconds); TI_2 , the second inversion time, ranging from 1.05 seconds to 4.47 seconds (step-size 0.02 seconds); TR_{GRE} , the gradient echo repetition time, equal to 5.6 ms; TR_{Seq} , the sequence repetition time, equal to 5 seconds and N_{Ex} , the number of excitations, equal to 144 ($6/8 \times$ number of slices).

2.2 | Contrast generation with the FLAWS sequence

The FLAWS-uni image was reconstructed by default by the MR system, with:

$$S_{uni} = \frac{\text{Real}(S1_C^* S2_C)}{|S1_C|^2 + |S2_C|^2} \quad (1)$$

where $S1_C$ (respectively $S2_C$) denote the complex signal of FLAWS1 (respectively FLAWS2), and * designs the complex conjugate.

The signal of the FLAWS minimum image (FLAWS-min), characterized by the suppression of both WM and CSF signals, was computed as follows⁸:

$$S_{min} = \frac{\min(S1, S2)}{S1 + S2} \quad (2)$$

with $S1$ and $S2$ the magnitude of the FLAWS1 and FLAWS2 signals, respectively. The signal of FLAWS-hc was computed using the following equation¹⁸:

$$S_{hc} = \frac{S1 - S2}{S1 + S2} \quad (3)$$

Because of the design of the FLAWS sequence, the FLAWS-uni, FLAWS-min, and FLAWS-hc signals are independent from the T_2^* relaxation, M_0 , and B_1^- .^{2,18}

The contrast of FLAWS-hc is similar to the contrast of FLAWS1, with a suppression of the WM signal.¹⁸ A bias-reduced standard T_1 -weighted contrast can be obtained by computing the opposite of FLAWS-hc, named FLAWS-hco:

$$S_{hco} = \frac{S2 - S1}{S1 + S2} \quad (4)$$

The reconstruction of the FLAWS-min, FLAWS-hc, and FLAWS-hco images from the magnitude of the FLAWS1 and FLAWS2 signals leads to a loss of contrast compared with image reconstructions from complex signals. The contrast lost from the magnitude reconstruction was recovered using the sign information of the FLAWS-uni signal (refer to the Supplementary Materials for more information).

FLAWS-uni, FLAWS-min, FLAWS-hc, and FLAWS-hco are characterized by an enhanced background noise¹⁸ and were denoised by adding coefficients in the image combinations.²⁰

2.3 | T_1 mapping with the FLAWS sequence

Providing that FLAWS-hc is independent from the T_2^* relaxation, M_0 , and B_1^- ,¹⁸ the T_1 relaxation time should be measurable with the FLAWS sequence using lookup tables of the FLAWS-hc signal. The FLAWS-hc signal was reconstructed offline using the magnitude of the FLAWS1 and FLAWS2 signals. This leads to T_1 -mapping ambiguities, as FLAWS1 and FLAWS2 signals with opposite signs would have the same intensity in FLAWS-hc, though they correspond to signals with different T_1 relaxation times. The T_1 -mapping ambiguities induced by the FLAWS-hc signal were solved using the sign information of the FLAWS-uni signal (refer to the Supplementary Materials section, *Contrast loss and T_1*

TABLE 1 Proposed FLAWS sequence parameters for 7T imaging

Sequence	FLAWS	MP2RAGE	SA2RAGE
TR/TE (ms)	5000/2.04	6000/2.16	2400/0.95
TI (ms)	620/1430	800/2700	106/1800
Flip angles	4°/8°	3°/4°	6°/10°
Matrix	300 × 300	240 × 240	64 × 64
Slices	192	160	48
Resolution (mm ³)	0.8 × 0.8 × 0.8	1.0 × 1.0 × 1.0	4.0 × 4.0 × 4.0
BW (Hz/px)	370	300	490
Orientation	Sagittal	Sagittal	Sagittal
FOV (mm ²)	240 × 240	240 × 240	256 × 232
GRAPPA	3	3	None
Slice partial Fourier	6/8	6/8	6/8
Scan time (min:s)	10:02	10:02	1:28

The parameters used to acquire the MP2RAGE and SA2RAGE data in this study are also shown.

Abbreviations: BW, bandwidth; FLAWS, fluid and white matter suppression; FOV, field of view; GRAPPA, generalized auto-calibrating partially parallel acquisitions; MP2RAGE, magnetization-prepared two rapid gradient echoes; px, pixel; SA2RAGE, saturation-prepared with two rapid gradient echoes; TE, echo time; TI, inversion time; TR, sequence repetition time

mapping ambiguities and Supporting Information Figure S1 for more information).

2.4 | Simulation experiments

The effect of B_1^+ on the T_1 measurements provided by the FLAWS sequence was assessed using Monte-Carlo experiments. The signals of FLAWS1 and FLAWS2 were simulated as follows:

$$S1 = f_1(\Gamma_{B1^+} \times \alpha_1, \Gamma_{B1^+} \times \alpha_2, TI_1, TI_2, TR_{GRE}, TR_{Seq}, N_{Ex}, t1) + \sigma_{N1} \quad (5)$$

$$S2 = f_2(\Gamma_{B1^+} \times \alpha_1, \Gamma_{B1^+} \times \alpha_2, TI_1, TI_2, TR_{GRE}, TR_{Seq}, N_{Ex}, t1) + \sigma_{N2} \quad (6)$$

with f_1 (respectively f_2) a function determined by solving the Bloch equations of the FLAWS sequence to simulate FLAWS1 (respectively FLAWS2) signal at the center of the k-space. Γ_{B1^+} is a random variable following a gamma distribution tailored to fit the brain B_1^+ values measured in the current study (refer to the Supplementary Materials for more information). The random variables σ_{N1} and σ_{N2} follow a normal distribution with a mean of 0 and a standard deviation of $S2_{WM}/25$ to simulate FLAWS images with a SNR of 25.

Monte Carlo experiments were performed for every T_1 value ranging from 900 to 2500 ms (step-size: 1 ms) by simulating 1000 FLAWS signals per T_1 value. These Monte-Carlo experiments were used to compute the theoretical accuracy and precision of the FLAWS T_1 mapping (mathematical equations provided in Supplementary Materials).

To decouple the effect of the SNR and the B_1^+ on the T_1 mapping, the theoretical accuracy and precision of the T_1

measurements were computed in three different simulation cases: (1) signals simulated with a SNR of 25 and without B_1^+ ($\Gamma_{B1^+} = 1$); (2) signals simulated with an infinite SNR ($\sigma_{N1} = \sigma_{N2} = 0$) and with B_1^+ ; and (3) signals simulated with a SNR of 25 and with B_1^+ .

For comparison, the theoretical accuracy and precision of the MP2RAGE T_1 mapping were computed by simulating Monte-Carlo experiments with the same B_1^+ and noise distributions as the ones used to simulate FLAWS data.

2.5 | In vivo experiments

2.5.1 | MRI acquisition

Experiments were performed on six healthy volunteers (21 to 48 years of age, 2 women) with a 7T whole-body MRI research scanner (Siemens Healthcare, Erlangen, Germany) equipped with a 32-channel head coil (Nova Medical, Wilmington, DE). All experiments were performed under written informed consent and were approved by the institutional review board (University of Queensland Human Research Ethics Committee A - approval number 2018001588).

A B_1^+ map was acquired for each volunteer using the SA2RAGE sequence.²¹ Then, MP2RAGE and FLAWS images were acquired. The MP2RAGE sequence was acquired with parameters that had been optimized to obtain an MP2RAGE-uni signal with low B_1^+ sensitivity.⁶ The FLAWS parameters were those obtained from the optimization outlined in the current study. It should be noted that the MP2RAGE optimization⁶ used in this study provided a lower resolution (1 mm isotropic) than the FLAWS optimization

(0.8 mm isotropic). The parameters used for the SA2RAGE, MP2RAGE, and FLAWS acquisitions are presented in Table 1.

2.5.2 | FLAWS sequence optimization and contrast generation

The optimized 7T FLAWS sequence was qualitatively and quantitatively assessed using in vivo experiments on healthy volunteers. To be consistent with the qualitative assessments performed in previous FLAWS optimization studies,^{8,9} the images acquired in the current study were reviewed to ensure that the separation between the external globus pallidus (GPe) and the internal globus pallidus (GPi) was clearly identified in FLAWS1. The quantitative assessment was performed by measuring the contrast (CN) and CNR per unit of time between brain tissues in FLAWS1 and FLAWS2. The CN and CNR were computed as follows:

$$CN_{A/B} = \frac{|S_A - S_B|}{|S_A| + |S_B|} \quad (7)$$

$$CNR_{A/B} = \frac{|S_A - S_B|}{\sqrt{\frac{\sigma_A^2 + \sigma_B^2}{2}}} \times \frac{1}{\sqrt{TR}} \quad (8)$$

with S_A (respectively S_B) and σ_A (respectively σ_B) the mean and the standard deviation of a given tissue A (respectively B) and TR the sequence repetition time. The means and standard deviations of WM, GM, and CSF were, respectively, measured in regions of interest (ROIs) manually drawn in the corpus callosum (splenium), the caudate nucleus (head), and the lateral ventricles. The SNR of WM was measured in FLAWS2 using the following equation:

$$SNR = \frac{S2_W}{\sigma 2_W} \quad (9)$$

with $S2_W$ and $\sigma 2_W$ the mean and the standard deviation of the WM signal in FLAWS2.

The CNs and CNRs between brain tissues of FLAWS-uni, FLAWS-min, and FLAWS-hco were measured in vivo and compared with the CNs and CNRs measured in FLAWS1 and FLAWS2. The CN and CNR values of FLAWS-hc are not presented in this article as they are equal to the CN and CNR values of FLAWS-hco ($S_{hc} = -1 \times S_{hco}$). The CNs and CNRs of MP2RAGE-uni, generated with the MP2RAGE sequence, were also computed. To compare the MP2RAGE-uni and FLAWS-hco CNRs, though MP2RAGE-uni and FLAWS-hco are characterized by different resolutions, specific care was

taken to ensure that no partial volume voxels were included in the ROIs used to compute the CNR.

2.5.3 | T₁ mapping

The SA2RAGE data was spatially normalized on the MP2RAGE and FLAWS data by registering the second 3D dataset to the second MP2RAGE and FLAWS 3D datasets. The registrations were performed using a block-matching rigid registration algorithm (Anima, RRID:SCR_017017; <https://github.com/Inria-Visages/Anima-Public>).^{22,23} The MP2RAGE data were spatially normalized on the FLAWS data using the same process.

MP2RAGE and FLAWS T₁ maps were B₁⁺ corrected using the B₁⁺ map provided by the SA2RAGE sequence using the method described in Marques and Gruetter.⁶ In vivo T₁ relaxation times of WM, putamen, caudate nucleus, and cortical GM were measured by manually drawing ROIs within the MP2RAGE and FLAWS T₁ maps. For more information about the selection of the ROIs, please refer to Wright et al.²⁴

MP2RAGE and FLAWS data were segmented using a similar approach as in Haast et al.⁷ First, the MP2RAGE and FLAWS second 3D datasets were bias corrected using the N4 algorithm from Tustison et al.²⁵ Then, the bias-corrected images were skull-stripped using FSL-Bet2,²⁶ and the brain masks were used to remove all nonbrain tissues in MP2RAGE-uni and FLAWS-hco. Finally, the skull-stripped MP2RAGE-uni and FLAWS-hco images were segmented with FreeSurfer 6.0.²⁷

The Pearson's correlation between the MP2RAGE and FLAWS T₁ measurements was computed for every T₁ measured within brain tissue (CSF excluded) of the healthy volunteers. The average in vivo precision of the T₁ mapping (mathematical equation provided in Supplementary Materials) was computed within the WM and cortical GM segmentations provided by FreeSurfer. The effect of the B₁⁺ on the MP2RAGE and FLAWS T₁ mapping was assessed in vivo by measuring the Pearson's correlation between T₁ and B₁⁺ maps within the WM and cortical GM segmentations provided by FreeSurfer.

3 | RESULTS

3.1 | Sequence optimization

The FLAWS sequence parameters optimized in the current study are presented in Table 1. The FLAWS1 (first 3D dataset, WM suppressed) and FLAWS2 (second 3D dataset, CSF suppressed) signals simulated with this optimized set of parameters are shown in Figure 1A. In FLAWS1, most of the WM signal is successfully suppressed, with strong

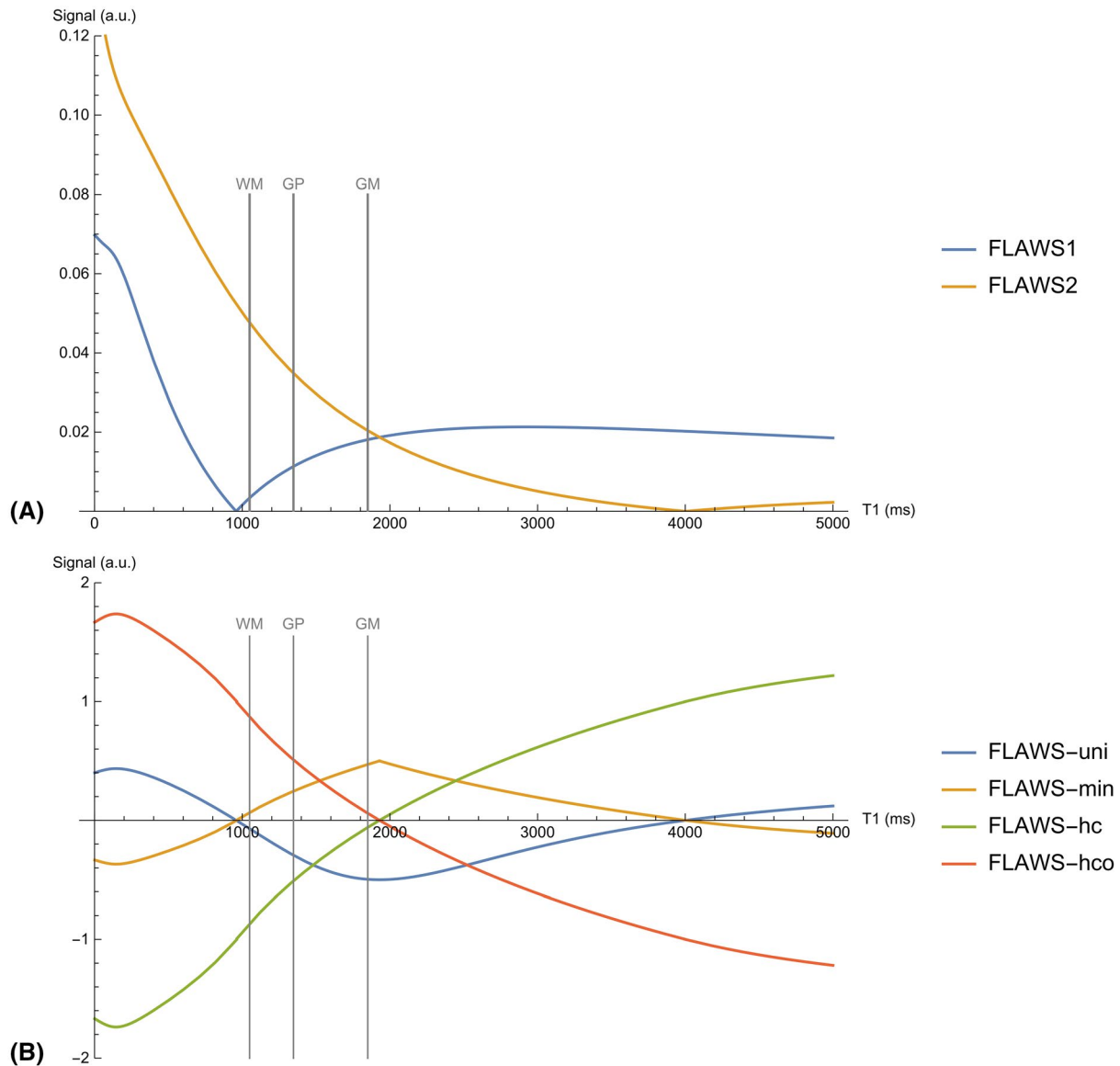


FIGURE 1 Simulations of the acquired (A) and reconstructed (B) fluid and white matter suppression (FLAWS) signals with the parameters optimized in the current study. GM, gray matter; GP, globus pallidus; WM, white matter

signals obtained from the globus pallidus, GM, and CSF. The FLAWS2 signal is successfully characterized by a strong CSF suppression, resulting in a high signal for WM and GM and good contrast between them.

An example of FLAWS images acquired at 7T with the set of parameters optimized in this study is shown in Figure 2. From a qualitative point of view, the FLAWS1 and FLAWS2 contrasts acquired at 7T in the current study look similar to the contrasts obtained with previous optimizations of the sequence at both 1.5T and 3T.^{8,9} A time of flight effect was found in FLAWS images, making the blood vessels appear hyperintense, as depicted in Figure 2B. However, the blood hyperintensity was found to vary with blood flow and could not be used to generate MR angiographies. A qualitative assessment validated the proposed 7T sequence parameters to visualize the basal ganglia in FLAWS1 images, which

provide a clear separation between the GPe and the GPi as shown in Supporting Information Figure S2.

The values of the brain tissue contrasts measured in vivo in the current study are reported in Table 2. For comparison, the brain tissue contrasts measured in the same ROIs for the 1.5T and 3T FLAWS optimizations are also reported.^{8,9} The CN values obtained in the current study agree with those obtained for the 1.5T and 3T studies. The average SNR of WM in FLAWS2 is equal to 25 ± 2 in the current study.

3.2 | Contrast generation with the FLAWS sequence

Simulations of the bias-reduced FLAWS-uni, FLAWS-min, FLAWS-hc, and FLAWS-hco signals are shown in Figure 1B

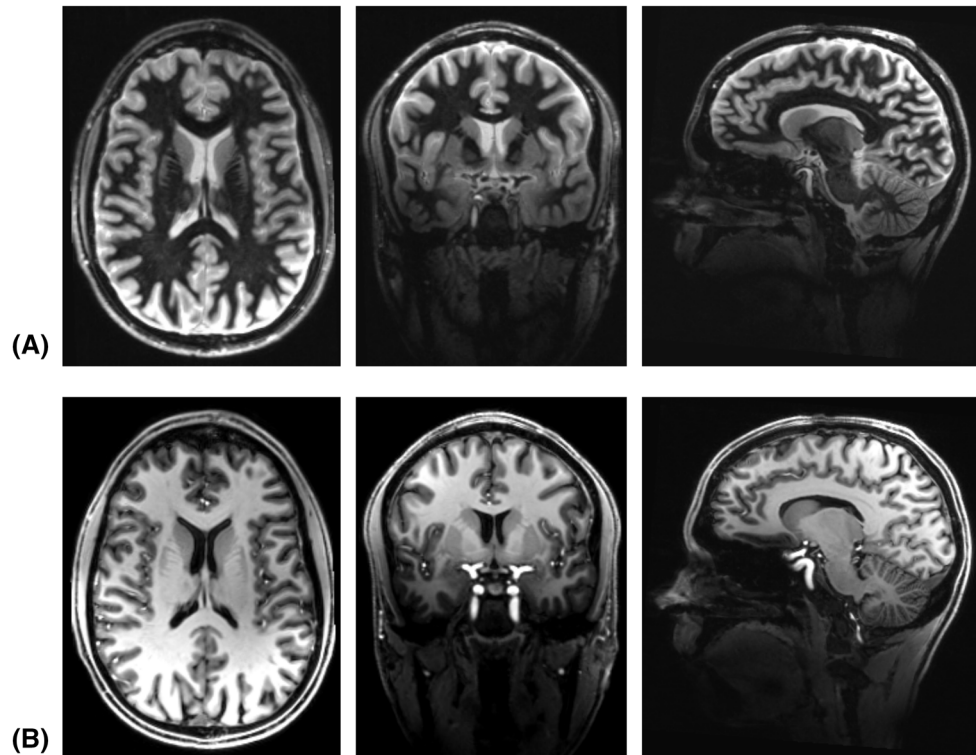


FIGURE 2 Axial (left), coronal (center), and sagittal (right) images of FLAWS1 (A) and FLAWS2 (B) acquired at 7T on one healthy volunteer with the set of parameters presented in Table 1

TABLE 2 In vivo measurements of the contrast of FLAWS images acquired at 7T with the set of parameters presented in Table 1

Contrast	FLAWS1			FLAWS2		
	1.5T	3T	7T	1.5T	3T	7T
WM/GM	0.69 (0.59-0.69)	0.59 (0.51-0.69)	0.68 (0.58-0.72)	0.23 (0.19-0.28)	0.15 (0.13-0.16)	0.25 (0.21-0.31)
WM/CSF	0.75 (0.67-0.89)	0.68 (0.62-0.77)	0.82 (0.77-0.85)	0.88 (0.82-0.93)	0.83 (0.68-0.89)	0.81 (0.76-0.86)
GM/CSF	0.12 (0.08-0.19)	0.16 (0.13-0.17)	0.32 (0.29-0.34)	0.81 (0.72-0.89)	0.78 (0.60-0.86)	0.70 (0.65-0.77)

For comparison, the values measured in the work by Beaumont et al at 1.5T⁹ and Tanner et al at 3T⁸ are also reported. The CN values of the FLAWS optimization proposed for 7T imaging are in agreement with the FLAWS CN obtained at 1.5T and 3T. CN measurements were performed in the corpus callosum (splenium) for WM, caudate nucleus (head) for GM, and lateral ventricle for CSF. The CN range is presented in parentheses.

Abbreviations: CN, Contrast; CSF, cerebrospinal fluid; FLAWS, fluid and white matter suppression; GM, gray matter; WM, white matter.

for the optimization proposed in the current study. Simulations indicate that FLAWS-uni is characterized by a low GM signal compared with its WM and CSF signals, thus suggesting that it provides a GM-suppressed contrast instead of providing the standard T_1 -weighted contrast typical from MP2RAGE-uni. FLAWS-min provides a high GM signal compared with the signals of WM and CSF. In accordance with previous theoretical experiments performed at 1.5T,⁹ the signal of the 7T FLAWS-hc-combination image is characterized by a WM-suppressed signal, with an increased contrast between GM and CSF compared to FLAWS1. Similarly, FLAWS-hco provides a CSF-suppressed signal with an increased contrast between WM and GM compared to FLAWS2. The assumptions deduced from signal simulations were confirmed by in

vivo imaging, as shown in Figure 3. The bias field reduction provided in vivo by FLAWS-uni, FLAWS-min, FLAWS-hc, and FLAWS-hco is noteworthy compared to FLAWS1 and FLAWS2 in Figure 3. This bias field reduction is further highlighted in Supporting Information Figure S3.

The CN and CNR measured in FLAWS1, FLAWS2, FLAWS-uni, FLAWS-min, FLAWS-hco, and MP2RAGE-uni are reported in Table 3. The results of the CN and CNR analysis show quantitatively that FLAWS-uni provides a GM-suppressed contrast, with high CN and CNR values measured for WM/GM and GM/CSF, compared with the CN and CNR values measured for WM/CSF. Similarly, the high CNR values obtained for WM/GM and GM/CSF compared to WM/CSF in FLAWS-min confirm quantitatively

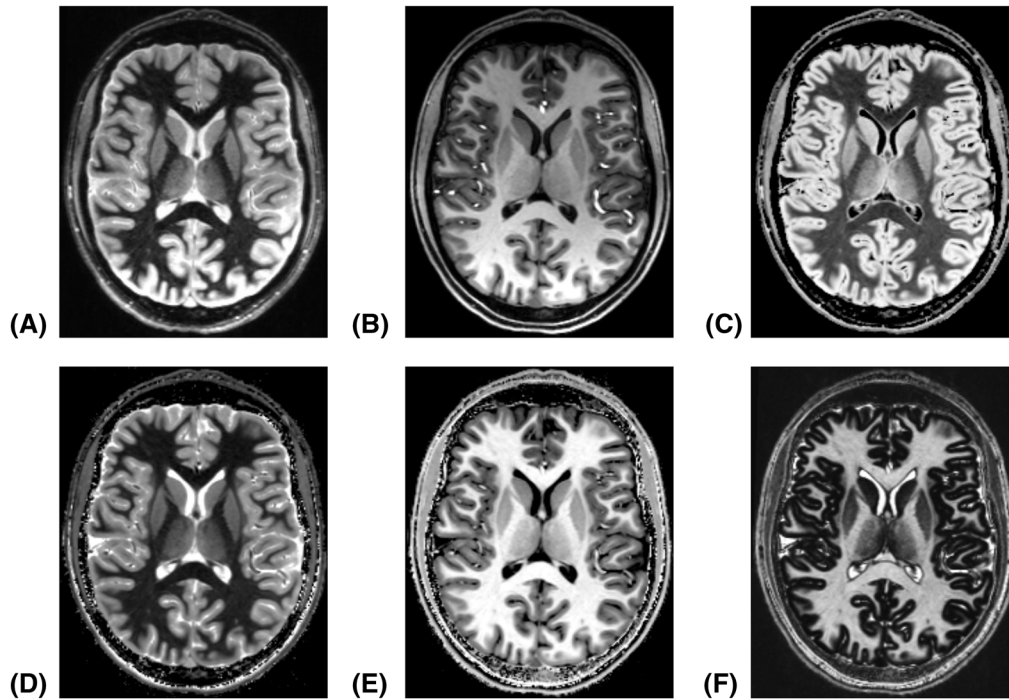


FIGURE 3 Example of the different contrasts obtained with fluid and white matter suppression (FLAWS) imaging at 7T. A, FLAWS1. B, FLAWS2. C, FLAWS-min. D, FLAWS-hc. E, FLAWS-hco. F, FLAWS-uni. FLAWS-min, FLAWS-hc, FLAWS-hco, and FLAWS-uni were denoised by adding coefficients in the image combinations²⁰

TABLE 3 Average contrast and contrast-to-noise ratio measured in vivo in FLAWS images acquired at 7T with the set of parameters presented in Table 1

		FLAWS1	FLAWS2	FLAWS-uni	FLAWS-min	FLAWS-hco	MP2RAGE-uni
CN	WM/GM	0.68 (0.58-0.72)	0.25 (0.21-0.31)	0.71 (0.63-0.77)	0.71 (0.62-0.76)	0.53 (0.47-0.58)	0.29 (0.25-0.31)
	WM/CSF	0.82 (0.77-0.85)	0.81 (0.75-0.86)	0.22 (0.19-0.25)	1.00 (1.00-1.00)	1.00 (1.00-1.00)	0.74 (0.68-0.82)
	GM/CSF	0.32 (0.29-0.34)	0.70 (0.63-0.77)	0.81 (0.76-0.85)	1.00 (1.00-1.00)	1.00 (1.00-1.00)	0.58 (0.49-0.68)
CNR	WM/GM	4.9 (3.6-5.9)	5.0 (4.0-6.1)	6.5 (5.2-7.8)	5.5 (4.6-6.1)	5.5 (4.6-6.1)	4.9 (3.7-6.4)
	WM/CSF	7.9 (4.6-9.7)	10.3 (7.5-13.9)	2.7 (2.0-3.2)	3.1 (2.3-3.7)	14.7 (12.8-16.6)	6.6 (5.4-8.1)
	GM/CSF	4.1 (2.6-5.1)	5.6 (4.4-7.0)	6.6 (5.6-8.2)	6.9 (5.6-8.5)	10.3 (8.2-12.0)	3.7 (2.4-4.6)

The average CN and CNR of the MP2RAGE images acquired in this study are also shown.

CN and CNR measurements were performed in the corpus callosum (splenium) for WM, caudate nucleus (head) for GM and lateral ventricle for CSF. Ranges of CN and CNR are presented in parentheses.

Abbreviations: CN, Contrast; CNR, contrast-to-noise ratio; CSF, cerebrospinal fluid; FLAWS, fluid and white matter suppression; GM, gray matter; MP2RAGE, magnetization-prepared two rapid gradient echoes; WM, white matter.

that FLAWS-min provides a GM-specific contrast. In agreement with previous studies performed at 1.5T,^{9,18} FLAWS-hco is characterized by an improved contrast with respect to FLAWS1 and FLAWS2, with a high CNR between brain tissues. In addition, FLAWS-hco is characterized by an enhanced CN compared with MP2RAGE-uni. FLAWS-hco also provides a higher CNR for WM/CSF and GM/CSF compared with MP2RAGE-uni. The WM/GM CNR measured in FLAWS-hco was close to the one measured in MP2RAGE-uni. The contrast enhancement provided by FLAWS-hco is noteworthy when compared

to MP2RAGE-uni, as shown in Supporting Information Figure S4.

3.3 | T₁ mapping

Simulations of the MP2RAGE-uni and FLAWS-hc signals affected by $\pm 40\%$ B₁⁺ inhomogeneities indicated that FLAWS-hc is robust to B₁⁺ inhomogeneities for the T₁ range of WM and GM signals, as shown in Supporting Information Figure S5. However, the sensitivity of the FLAWS-hc signal

to B_1^+ inhomogeneities increases for short (<1000 ms) and long (>2000 ms) T_1 relaxation times. Specifically, the FLAWS T_1 mapping theoretical error caused by $\pm 40\%$ B_1^+ inhomogeneities (4.3% for a T_1 of 2000 ms and 12.5% for a T_1 of 2500 ms) is higher than the one obtained from MP2RAGE optimized for reduced B_1^+ sensitivity (3.2% for a T_1 of 2000 ms and 4.4% for a T_1 of 2500 ms). The T_1 mapping theoretical error induced by $\pm 40\%$ B_1^+ inhomogeneities is, however, lower in FLAWS (4.3% for a T_1 of 2000 ms and 12.5% for a T_1 of 2500 ms) than in the MP2RAGE protocol optimized for high-resolution and high-contrast imaging (16.8% for a T_1 of 2000 ms and 24.7% for a T_1 of 2500 ms), whereas FLAWS is characterized by a higher resolution (0.8 mm isotropic) than this MP2RAGE protocol (0.85 mm isotropic).⁶

The high theoretical accuracy and precision of the T_1 maps obtained with the FLAWS and MP2RAGE sequences can be seen in Table 4. The results show that both the SNR and B_1^+ impact the accuracy and precision of the T_1 mapping. In all experiments, the average accuracy and precision of the FLAWS T_1 mapping were close to the ones of the MP2RAGE T_1 mapping, and were above 90% for the T_1 range of brain tissues (900 ms to 2500 ms).

Examples of in vivo T_1 maps—without post hoc correction—and B_1^+ maps obtained with the FLAWS, MP2RAGE, and SA2RAGE sequences are shown in Figure 4. From a qualitative point of view, the T_1 map provided by the FLAWS sequence looks like the MP2RAGE T_1 map and does not seem to be hampered by the B_1^+ . The difference between the MP2RAGE and FLAWS T_1 maps—without post hoc correction—appears to be mainly caused by the resolution difference between the scans, as shown in Supporting Information Figures S6 and S7

The effect of the post hoc correction on the in vivo FLAWS T_1 measurements appears to be negligible for most of the brain tissues, except for long T_1 relaxation times like cortical GM, as shown in Table 5. A slightly higher T_1 change was found in brain tissues regarding the B_1^+ correction of

MP2RAGE T_1 measurements, except for long T_1 relaxation times like cortical GM. The B_1^+ corrected T_1 measurements provided by the FLAWS sequence were in concordance with the ones provided by the MP2RAGE sequence optimized for low B_1^+ sensitivity ($r=0.91$). In addition, the B_1^+ corrected FLAWS T_1 measurements performed in this study provided results close to T_1 measurements performed in similar ROIs by T_1 curve fitting of MPRAGE data acquired at multiple inversion times in a previous study.²⁴

The average precision of the FLAWS in vivo T_1 mapping, computed within the WM and cortical GM segmentations after B_1^+ correction ($prec_{WM}=86.3 \pm 0.5\%$; $prec_{GM}=87.8 \pm 0.5\%$), was close to the one computed on MP2RAGE T_1 maps after B_1^+ correction ($prec_{WM}=87.9 \pm 0.3\%$; $prec_{GM}=83.8 \pm 3.1\%$).

The average in vivo T_1 values—without post hoc correction—measured with MP2RAGE and FLAWS within the WM and cortical GM segmentations of one volunteer were reported as a function of B_1^+ in Figure 5A,B. The effect of the B_1^+ on MP2RAGE and FLAWS T_1 mapping appears to be negligible for B_1^+ values within the 50 to 100% range for all volunteers. However, the T_1 values tend to diverge outside of this range. The divergence in the T_1 measurements was found to increase when the number of voxels per B_1^+ value decreases, as shown in Figure 5C,D. Across all the volunteers, 13.0% and 19.6% of the MP2RAGE WM and cortical GM voxels were characterized by a B_1^+ value outside of the 50 to 100% range. The rate of voxels outside of the 50 to 100% B_1^+ range was similar in FLAWS images (12.4% for WM and 17.0% for cortical GM). A qualitative assessment indicated that the voxels with a B_1^+ value under 50% of the nominal flip angles were located near the ear canals and the frontal sinuses, or were located in the inferior brain regions, where B_1^+ is characterized by a strong signal reduction in the z direction (example available in Supporting Information Figure S8). The voxels responsible for the T_1 mapping divergence for B_1^+ values over 100% of the nominal flip angles were found to be voxels misclassified at tissue boundaries (because of small errors in skull-stripping and segmentations; example available in Supporting Information Figure S9).

The average correlation between the T_1 relaxation time—measured without post-hoc correction—and the B_1^+ was weak within the WM and cortical GM segmentations for both MP2RAGE ($r_{WM}=-0.051 \pm 0.017$; $r_{GM}=-0.027 \pm 0.045$) and FLAWS ($r_{WM}=-0.026 \pm 0.021$; $r_{GM}=0.081 \pm 0.038$). The correlation remains weak when computed on voxels belonging to the 50 to 100% B_1^+ range within MP2RAGE ($r_{WM}=-0.040 \pm 0.040$; $r_{GM}=-0.040 \pm 0.036$) and FLAWS ($r_{WM}=-0.027 \pm 0.041$; $r_{GM}=-0.097 \pm 0.036$) segmentations. The bias correction of the T_1 maps slightly decreases the correlation between the T_1 relaxation time and the B_1^+ within the 50 to 100% range for both MP2RAGE

TABLE 4 Accuracy and precision of the T_1 measurements provided by the MP2RAGE sequence with low B_1^+ sensitivity and by the FLAWS sequence, according to different values of the signal-to-noise ratio and to the effect of the B_1^+ on the signal

Bias	SNR	Sequence	Accuracy (%)	Precision (%)
No B_1^+	25	MP2RAGE	93.7	92.1
		FLAWS	95.3	94.1
B_1^+	+∞	MP2RAGE	98.5	99.2
		FLAWS	96.4	97.8
	25	MP2RAGE	90.0	86.8
		FLAWS	91.9	90.2

Abbreviations: FLAWS, fluid and white matter suppression; MP2RAGE, magnetization-prepared two rapid gradient echoes.

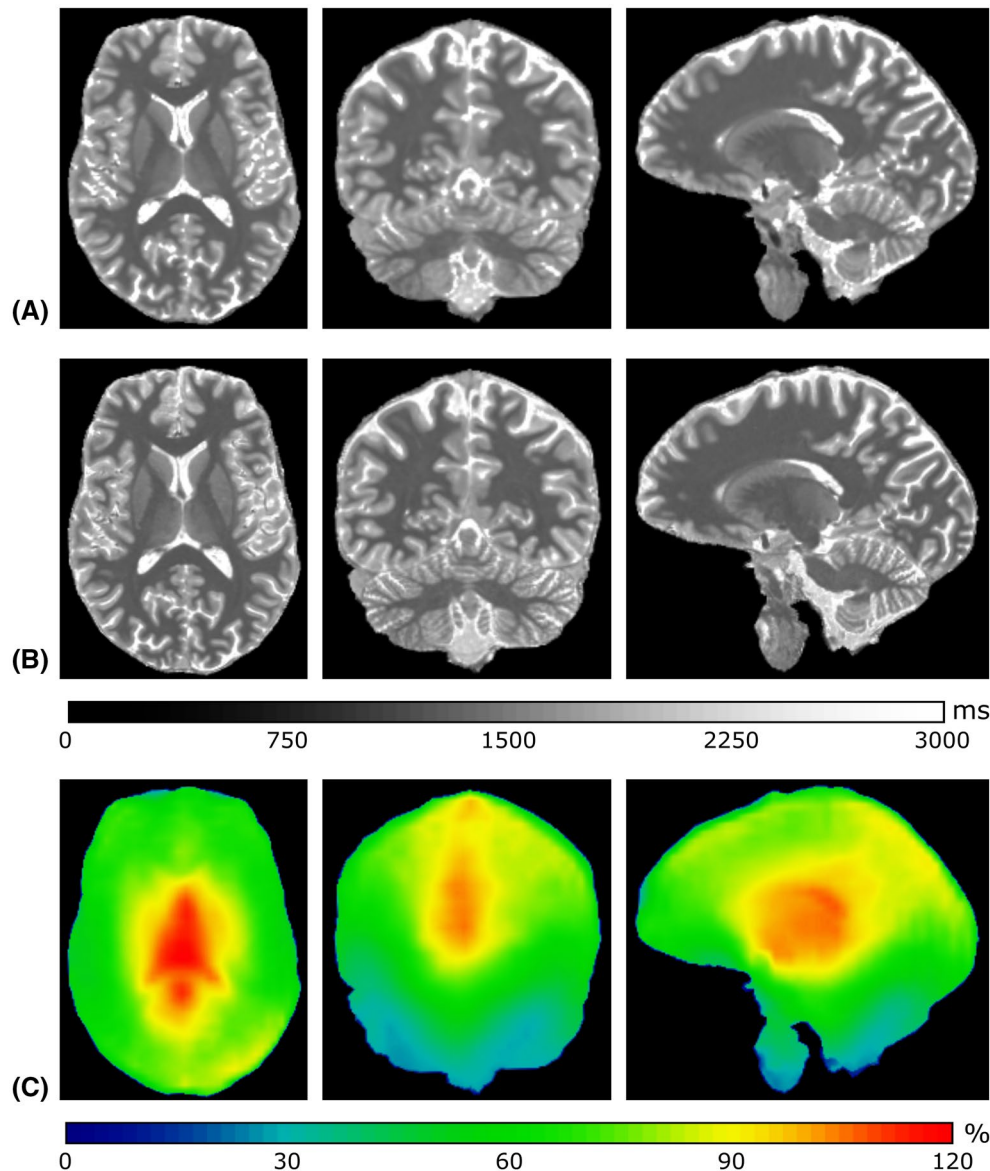


FIGURE 4 T_1 Maps—without post hoc B_1^+ correction—acquired with the magnetization-prepared two rapid gradient echoes (MP2RAGE) sequence optimized for low B_1^+ sensitivity (A) and with the fluid and white matter suppression (FLAWS) sequence optimized in this study (B). The B_1^+ map acquired with the saturation-prepared with two rapid gradient echoes (SA2RAGE) sequence of the same volunteer is also shown (C). The B_1^+ values are displayed as a percentage of the nominal sequence flip angles. From a qualitative point of view, the FLAWS and MP2RAGE T_1 maps are similar and do not appear to be sensitive to B_1^+

($r_{WM} = -0.011 \pm 0.035$; $r_{GM} = -0.013 \pm 0.027$) and FLAWS ($r_{WM} = -0.024 \pm 0.040$; $r_{GM} = -0.029 \pm 0.027$).

4 | DISCUSSION

4.1 | Sequence optimization

The FLAWS sequence was optimized at the field strength of 7T for high-resolution (0.8 mm isotropic) imaging using a method previously used to optimize the sequence at 1.5T.⁹ The 1.5T optimization process was customized to adapt the T_1 relaxation times, the sequence acquisition time, and image

resolution for 7T imaging. As the optimization method is based on simulations of brain tissue signals using the Bloch equations, the outcome of the optimization depends on the choice of the T_1 relaxation times used to simulate the signals.⁹ To increase the consistency between the FLAWS and MP2RAGE optimizations, the T_1 relaxation times used to optimize the FLAWS sequence were the same as the ones used to optimize the MP2RAGE sequence at 7T in a previous study.²

Simulations of FLAWS signals with the parameters optimized in this study indicate that the WM signal suppression is not perfect in FLAWS1. In a previous study performed at 3T, Tanner et al showed that the WM signal should not be

TABLE 5 Mean and standard deviation T_1 values measured in vivo on six healthy volunteers at 7T using the FLAWS sequence and the MP2RAGE sequence with low B_1^+ sensitivity

	FLAWS		MP2RAGE		Wright et al
	Raw	B_1^+ corr	Raw	B_1^+ corr	B_1^+ corr
White matter	1076 ± 40 ms	1071 ± 44 ms	1123 ± 41 ms	1110 ± 41 ms	1130 ± 100 ms
Caudate nucleus	1617 ± 83 ms	1615 ± 80 ms	1607 ± 74 ms	1598 ± 74 ms	1684 ± 76 ms
Putamen	1569 ± 78 ms	1569 ± 75 ms	1590 ± 70 ms	1578 ± 68 ms	1643 ± 167 ms
Cortical gray matter	1995 ± 128 ms	1941 ± 96 ms	1983 ± 134 ms	1954 ± 153 ms	1939 ± 150 ms

T_1 values are reported with (B_1^+ corr) and without (Raw) post hoc correction. T_1 values from the literature are also reported.²⁴ The T_1 values measured with FLAWS did not change after post hoc correction, except for tissues with long T_1 relaxation times, as cortical gray matter.

Abbreviations: FLAWS, fluid and white matter suppression; MP2RAGE, magnetization-prepared two rapid gradient echoes.

perfectly suppressed in FLAWS1 to ensure a good visualization of deep GM structures.⁸

The optimization method employed in this study was designed to provide a set of parameters to acquire 7T FLAWS images characterized by (1) a contrast similar to the one obtained with the 3T FLAWS sequence optimization,^{8,9} and (2) a good visualization of deep GM structures in FLAWS1. Qualitative and quantitative in vivo experiments showed that the optimization performed in this study provided images with a contrast similar to the one obtained in previous studies conducted at 1.5T and 3T.^{8,9} In addition, the separation between the GPe and the GPi—identified as a typical metric used to assess the quality of the basal ganglia visualization in FLAWS1^{8,9}—was clearly visible in the FLAWS1 images acquired with the set of parameters optimized in the current study.

4.2 | Contrast generation with the FLAWS sequence

The current study shows that “uni”, the image combination used to generate a bias-reduced standard T_1 -weighted contrast with MP2RAGE data, cannot provide a similar contrast with the proposed 7T FLAWS optimization. However, another image combination, named FLAWS-hco, was recently introduced at 1.5T to generate a bias-reduced standard T_1 -weighted contrast with the FLAWS sequence.⁹ Signal simulations, as well as qualitative and quantitative in vivo assessments, showed that FLAWS-hco provides a bias-reduced standard T_1 -weighted contrast for the FLAWS optimization proposed for 7T imaging. In addition, it was shown that the FLAWS-hco images acquired in the current study were characterized by an increased brain tissue CN, CNR, and resolution compared with the MP2RAGE-uni images acquired with parameters optimized for low B_1^+ sensitivity. Signal simulations, qualitative and quantitative in vivo assessments also showed that bias-reduced WM-suppressed, GM-suppressed, and GM-specific contrasts can be generated with 7T FLAWS

imaging, thus, allowing for the provision of more contrasts than the ones currently provided by the MP2RAGE sequence.

It should be noted that different MP2RAGE optimizations provide images with better CNR and resolution than the MP2RAGE optimization employed in the current study.⁶ However, these optimizations provide data with high B_1^+ sensitivity and could not be used as references to assess the B_1^+ sensitivity of the FLAWS optimization proposed in the current study.

4.3 | T_1 mapping

The current study shows that the FLAWS-hc signal can be used to measure the T_1 relaxation time. The theoretical accuracy and precision of FLAWS T_1 mapping were compared to the ones of the MP2RAGE T_1 mapping in terms of robustness to noise and B_1^+ . The consistency between the theoretical and in vivo experiments was ensured by simulating MP2RAGE and FLAWS signals with noise and B_1^+ distributions determined from the in vivo data acquired in this study.

Simulation experiments suggest that the proposed 7T FLAWS optimization can be used for accurate T_1 mapping with a low B_1^+ sensitivity and provides a theoretical accuracy and precision in agreement with the ones provided by the MP2RAGE sequence optimized for low B_1^+ sensitivity for the T_1 range of WM and GM tissues. These theoretical assumptions were supported by in vivo experiments showing that the FLAWS T_1 mapping provides T_1 measurements in agreement with the ones provided by other established T_1 mapping methods at 7T.^{2,24} In addition, the harmony observed between the in vivo FLAWS and MP2RAGE T_1 mapping precisions further validated the possibility of measuring T_1 relaxation times with the FLAWS sequence.

The small in vivo T_1 change noticed between the raw and post hoc corrected T_1 measurements provided by the MP2RAGE and FLAWS sequences suggests that FLAWS T_1 mapping is characterized by a low B_1^+ sensitivity for most brain tissues. The weak correlation between the B_1^+ and T_1

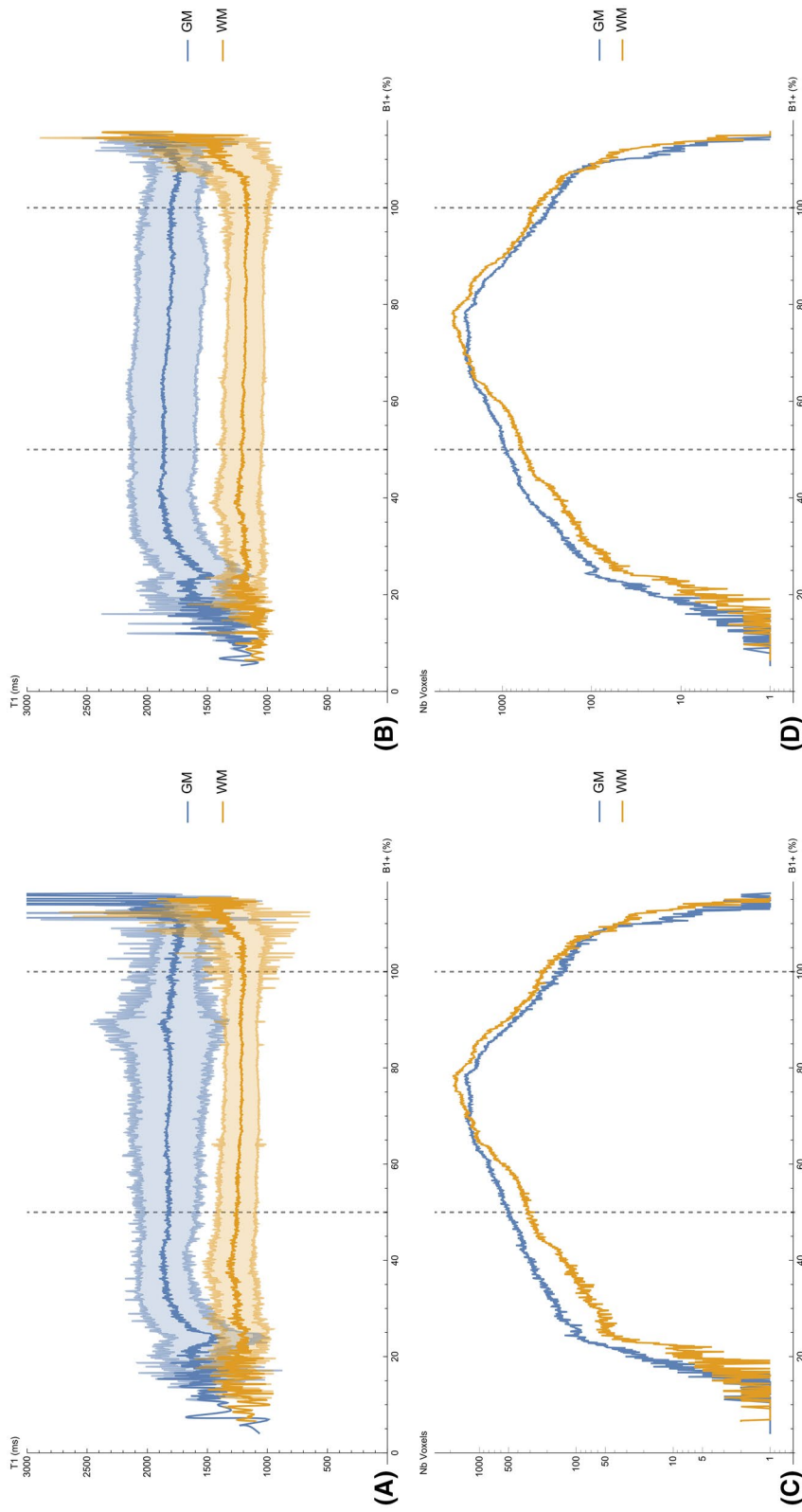


FIGURE 5 Effect of the transmitted bias field (B_1^+) on T_1 measurements—without post hoc correction—performed in vivo within white matter (WM) and cortical gray matter (GM); segmentations of one volunteer with the magnetization-prepared two rapid gradient echoes (MP2RAGE; A,C) and fluid and white matter suppression (FLAWS; B,D) sequences. First row: Average (dark color) and standard deviation (light color) of the WM and cortical GM MP2RAGE (A) and FLAWS (B) T_1 values as a function of B_1^+ . Second row: Number of voxels within the MP2RAGE (C) and FLAWS (D) WM and cortical GM segmentations as a function of B_1^+ . The B_1^+ values are displayed as a percentage of the nominal sequence flip angles

values—without post hoc correction—measured within WM and cortical GM segmentations with MP2RAGE and FLAWS further demonstrated the low B_1^+ sensitivity provided by the FLAWS optimization proposed in this study. However, it was shown that the FLAWS T_1 mapping is hampered by B_1^+ in cortical GM. Simulations of the FLAWS-hc signal hampered by B_1^+ inhomogeneities of $\pm 40\%$ indicated that the B_1^+ dependency of the FLAWS T_1 mapping increases for short (<1000 ms) and long (>2000 ms) T_1 relaxation times, thus, explaining the increased B_1^+ dependency of cortical GM, which is characterized by a long T_1 relaxation time compared with WM and deep GM. This increased dependency to B_1^+ for cortical GM signals was also found in the MP2RAGE T_1 mapping.

In agreement with previous studies conducted with MP2RAGE at 7T,^{6,7} the current study showed that the MP2RAGE T_1 maps can be post hoc corrected to remove the remaining bias in MP2RAGE data. The decreased correlation noticed between B_1^+ and T_1 for the FLAWS sequence after B_1^+ correction indicates that the method previously proposed by Marques et al⁶ to correct the B_1^+ in MP2RAGE-uni can also be used to correct the B_1^+ in FLAWS-hc. In a recent study, Haast et al assessed the effect of B_1^+ on multicenter MP2RAGE T_1 mapping and morphometry at 7T.²⁸ The authors advised to use MP2RAGE sequence parameters optimized for low B_1^+ sensitivity to improve the robustness of multicenter analysis, except when a good visualization of deep GM is required. To the best of our knowledge, the current study is the first that proposes a sequence optimization to acquire T_1 -weighted scans and T_1 maps characterized by a low B_1^+ sensitivity, while providing a good visualization of deep GM structures. Therefore, the results of the current study highlight the interest of FLAWS imaging to study deep GM in multicenter studies conducted at 7T.

This study shows that the T_1 relaxation times measured within WM and cortical GM segmentations tend to diverge for B_1^+ values outside of the 50 to 100% nominal flip angle range. A qualitative assessment showed that the low B_1^+ values were measured in the inferior brain regions, where the adiabatic condition of the inversion pulse might not be reached. This issue has already been reported in previous studies,^{6,7} and can be mitigated by placing dielectric pads near the temporal lobes.²⁹ Indeed, a previous study conducted with the MP2RAGE sequence showed that the use of dielectric pads increases the B_1^+ by up to 50% of the nominal flip angle near the cerebellum and the temporal lobes at 7T.³⁰ Low B_1^+ values were also found near the frontal sinuses and the ear canals. The presence of these low B_1^+ values could be explained by off-resonance frequency effects that are commonly found near the frontal sinuses and ear canals in B_1^+ mapping techniques.^{31,32} The high B_1^+ values that led to a divergence of the T_1 measurements within the WM and cortical GM segmentations were only noticed in voxels that were misclassified

as belonging to the WM or cortical GM segmentations. In addition, high B_1^+ values were measured in deep GM structures (see Figure 4C), where the effect of the B_1^+ correction on FLAWS T_1 mapping was shown to be negligible. Therefore, the T_1 divergence reported for high B_1^+ value in the current study was not considered as a failure of the MP2RAGE and FLAWS T_1 mapping methods.

4.4 | Limitations

The current study has several limitations. First, the MR experiments were performed on a small number of healthy volunteers: FLAWS imaging on a larger patient cohort would be necessary to assess the potential clinical interest provided by the multiple FLAWS contrasts for 7T imaging. In addition, the signals of FLAWS1 and FLAWS2 are dependent upon the number of slices; hence, a new optimization of the FLAWS sequence would be necessary to increase the scan resolution. Moreover, the bias-reduced FLAWS-min, FLAWS-hc, and FLAWS-hco combination images, as well as the FLAWS T_1 mapping, are not yet readily available on the MRI console. The code used to generate the FLAWS contrasts and perform the FLAWS T_1 mapping is, however, available on GitHub (<https://github.com/jerbeaumont/FLAWS-Tools>). Finally, the B_1^+ dependency of the FLAWS T_1 mapping increases for long T_1 and as such, a B_1^+ post hoc correction of the FLAWS T_1 maps is necessary to study tissues with long T_1 relaxation times, such as brain lesions.

5 | CONCLUSION

In conclusion, this study proposes a new optimization of the FLAWS sequence to provide multiple T_1 -weighted contrasts with reduced B_1 sensitivity that might be of interest for high-resolution (0.8 mm isotropic) 7T imaging. It was shown that the proposed FLAWS optimization provides high-resolution T_1 maps with low B_1^+ sensitivity, thus, overcoming the limitations of the MP2RAGE sequence optimized for low B_1^+ sensitivity in terms of CNR and resolution. These results suggest that FLAWS is a good candidate for T_1 -weighted imaging and T_1 mapping at the field strength of 7T.

ACKNOWLEDGMENTS

We thank the “Region Bretagne” (France), which partially funded the current study. We would also like to thank Siemens Healthcare for providing the MP2RAGE WIP 944, which allowed us to perform the experiments on the scanner. We acknowledge the facilities and the scientific and technical assistance of the National Imaging Facility at the Centre for Advanced Imaging, University of Queensland, Australia.

DATA AVAILABILITY STATEMENT

The code that supports the findings of this study is openly available in the FLAWS-Tools repository at <https://github.com/jerbeaumont/FLAWS-Tools.git> (<https://doi.org/10.5281/zenodo.3993247>).

ORCID

Jérémy Beaumont  <https://orcid.org/0000-0003-1198-2217>

REFERENCES

- Trattnig S, Springer E, Bogner W, et al. Key clinical benefits of neuroimaging at 7 T. *Neuroimage*. 2018;168:477-489.
- Marques JP, Kober T, Krueger G, van der Zwaag W, Van de Moortele P-F, Gruetter R. MP2RAGE, a self bias-field corrected sequence for improved segmentation and T1-mapping at high field. *Neuroimage*. 2010;49:1271-1281.
- Okubo G, Okada T, Yamamoto A, et al. MP2RAGE for deep gray matter measurement of the brain: A comparative study with MPRAGE. *J Magn Reson Imaging*. 2016;43:55-62.
- Kober T, Granziera C, Ribes D, et al. MP2RAGE multiple sclerosis magnetic resonance imaging at 3 T. *Invest Radiol*. 2012;47:346-352.
- Simioni S, Amarù F, Bonnier G, et al. MP2RAGE provides new clinically-compatible correlates of mild cognitive deficits in relapsing-remitting multiple sclerosis. *J Neurol*. 2014;261:1606-1613.
- Marques JP, Gruetter R. New developments and applications of the MP2RAGE sequence—Focusing the contrast and high spatial resolution R1 mapping Yacoub E, editor. *PLoS One*. 2013;8:e69294.
- Haast RAM, Ivanov D, Uludağ K. The impact of B1+ correction on MP2RAGE cortical T₁ and apparent cortical thickness at 7T. *Hum Brain Mapp*. 2018;39:2412-2425.
- Tanner M, Gambarota G, Kober T, et al. Fluid and white matter suppression with the MP2RAGE sequence. *J Magn Reson Imaging*. 2012;35:1063-1070.
- Beaumont J, Saint-Jalmes H, Acosta O, et al. Multi T1-weighted contrast MRI with fluid and white matter suppression at 1.5 T. *Magn Reson Imaging*. 2019;63:217-225.
- Mugler JP, Brookeman JR. Three-dimensional magnetization-prepared rapid gradient-echo imaging (3D MP RAGE). *Magn Reson Med*. 1990;15:152-157.
- Redpath TW, Smith FW. Use of a double inversion recovery pulse sequence to image selectively grey or white brain matter. *Br J Radiol*. 1994;67:1258-1263.
- Geurts JGG, Pouwels PJW, Uitdehaag BMJ, Polman CH, Barkhof F, Castelijns JA. Intracortical lesions in multiple sclerosis: Improved detection with 3D double inversion-recovery MR imaging. *Radiology*. 2005;236:254-260.
- Urushibata Y, Kuribayashi H, Fujimoto K, et al. Advantages of fluid and white matter suppression (FLAWS) with MP2RAGE compared with double inversion recovery turbo spin echo (DIR-TSE) at 7T. *Eur J Radiol*. 2019;116:160-164.
- Chen X, Qian T, Kober T, et al. Gray-matter-specific MR imaging improves the detection of epileptogenic zones in focal cortical dysplasia: A new sequence called fluid and white matter suppression (FLAWS). *NeuroImage Clin*. 2018;20:388-397.
- Bannier E, Gambarota G, Ferre J-C, et al. FLAWS imaging improves depiction of the thalamic subregions for DBS planning in epileptic patients. In: The International Society for Magnetic Resonance in Medicine (ISMRM). 2018. Abstract 0313.
- Martin-Bastida A, Ward RJ, Newbould R, et al. Brain iron chelation by deferiprone in a phase 2 randomised double-blinded placebo controlled clinical trial in Parkinson's disease. *Sci Rep*. 2017;7:1398.
- Wang Y, Wang Y, Zhang Z, et al. Segmentation of gray matter, white matter, and CSF with fluid and white matter suppression using MP2RAGE. *J Magn Reson Imaging*. 2018;48:1540-1550.
- Beaumont J, Saint-Jalmes H, Acosta O, et al. High contrast T1-weighted MRI with fluid and white matter suppression using MP2RAGE. In: IEEE International Symposium on Biomedical Imaging. Venice, Italy; 2019, pp. 701-704.
- Rooney WD, Johnson G, Li X, et al. Magnetic field and tissue dependencies of human brain longitudinal H₂O relaxation in vivo. *Magn Reson Med*. 2007;57:308-318.
- O'Brien KR, Kober T, Hagmann P, et al. Robust T1-weighted structural brain imaging and morphometry at 7T using MP2RAGE. *PLoS ONE*. 2014;9:e99676.
- Eggenschwiler F, Kober T, Magill AW, Gruetter R, Marques JP. SA2RAGE: A new sequence for fast B1+-mapping. *Magn Reson Med*. 2012;67:1609-1619.
- Commowick O, Wiest-Daessle N, Prima S. Block-matching strategies for rigid registration of multimodal medical images. In: 2012 9th IEEE International Symposium on Biomedical Imaging (ISBI). IEEE; 2012, pp. 700-703.
- Ourselin S, Roche A, Prima S, Ayache N. *Block Matching: A General Framework to Improve Robustness of Rigid Registration of Medical Images*. Berlin, Heidelberg: Springer; 2000, pp. 557-566.
- Wright PJ, Mougin OE, Totman JJ, et al. Water proton T₁ measurements in brain tissue at 7, 3, and 1.5T using IR-EPI, IR-TSE, and MPRAGE: Results and optimization. *Magn Reson Mater Physics, Biol Med*. 2008;21:121-130.
- Tustison NJ, Avants BB, Cook PA, et al. N4ITK: Improved N3 bias correction. *IEEE Trans Med Imaging*. 2010;29:1310-1320.
- Jenkinson M, Beckmann CF, Behrens TEJ, Woolrich MW, Smith SM. FSL. *Neuroimage*. 2012;62:782-790.
- Fischl B. FreeSurfer. *Neuroimage*. 2012;62:774-781.
- Haast RA, Lau JC, Ivanov D, Menon RS, Uludağ K, Khan AR. Effects of MP2RAGE B1+ sensitivity on inter-site T1 reproducibility and morphometry at 7T. *bioRxiv* 2020:2020.02.13.947382.
- Teeuwisse WM, Brink WM, Webb AG. Quantitative assessment of the effects of high-permittivity pads in 7 Tesla MRI of the brain. *Magn Reson Med*. 2012;67:1285-1293.
- O'Brien KR, Magill AW, Delacoste J, et al. Dielectric pads and low- B1+ adiabatic pulses: Complementary techniques to optimize structural T_{1w} whole-brain MP2RAGE scans at 7 Tesla. *J Magn Reson Imaging*. 2014;40:804-812.
- Duan Q, van Gelderen P, Duyn J. Improved Bloch-Siegert based B₁ mapping by reducing off-resonance shift. *NMR Biomed*. 2013;26:1070-1078.
- Wang J, Mao W, Qiu M, Smith MB, Constable RT. Factors influencing flip angle mapping in MRI: RF pulse shape, slice-select gradients, off-resonance excitation, and B0 inhomogeneities. *Magn Reson Med*. 2006;56:463-468.

SUPPORTING INFORMATION

Additional Supporting Information may be found online in the Supporting Information section.

FIGURE S1 Simulations of the FLAWS1 and FLAWS2 real parts of the complex signals (A). Simulations of the reconstructed FLAWS signals are shown in (B). $S1_0$: sign change in FLAWS1. $S2_0$: sign change in FLAWS2. The sign of FLAWS-uni is linked to the sign change of FLAWS1 and FLAWS2. A loss of contrast is noticed in FLAWS-hc, FLAWS-hco and FLAWS-min at every sign change ($S1_0$, $S2_0$)

FIGURE S2 Visualization of the separation between the internal and the external globus pallidus in FLAWS1. The separation is indicated by the white arrow

FIGURE S3 Illustration of the bias field reduction provided by FLAWS-hc (B) and FLAWS-hco (d) compared to FLAWS1 (A) and FLAWS2 (C)

FIGURE S4 Example of axial, coronal and sagittal images of MP2RAGE-uni (A) and FLAWS-hco (B). The increased contrast and resolution provided by FLAWS-hco is noteworthy

FIGURE S5 T1 relaxation time as a function of MP2RAGE-uni (blue line) and FLAWS-hc (orange line). The comparison is performed for MP2RAGE signals from the reduced B_1^+ MP2RAGE optimization (A), the high WM/GM contrast MP2RAGE optimization (B) and the high resolution MP2RAGE optimization (C) presented in Marques et al, Plos one, 2013 [6]. The dashed lines show the signals affected by $\pm 40\%$ B_1^+ inhomogeneities. This figure shows that FLAWS-hc is robust to B_1^+ inhomogeneities for the T1 range of WM and GM signals (gray zone). However, the sensitivity of the FLAWS-hc signal to B_1^+ inhomogeneities increases for short (<1000 ms) and long (>2000 ms) T1 relaxation times. It should be noted that the proposed FLAWS optimization allows to maintain a reduced B_1^+ sensitivity for FLAWS-hc signals acquired with a high number of excitations ($nEx = 144$) compared to the MP2RAGE optimizations previously proposed at 7T for high WM/GM contrast ($nEx = 132$, b) or high (0.65 mm isotropic) resolution ($nEx = 192$, c). The MP2RAGE-uni signal was plotted on the $[-1; 1]$ range to allow a comparison with the FLAWS-hc signal. The full range MP2RAGE-uni signal was recovered using the division image for the high WM/GM contrast protocol, as suggested in [6]

FIGURE S6 Example of MP2RAGE (A) and FLAWS (C) T1 maps without post-hoc correction. The difference between the T1 maps (B) appears to be mostly due to the T1 measurements of the CSF. A qualitative assessment suggested that most of the differences found for WM and GM tissues were due to the resolution difference between the two scans, as

illustrated in the zoomed-in version of this figure presented in Supporting Information Figure S7. The difference between the MP2RAGE and FLAWS T1 maps did not appear to be mainly impacted by the changes in the B_1^+ map (D)

FIGURE S7 Example of MP2RAGE (A) and FLAWS (C) T1 maps without post-hoc correction. The difference between the MP2RAGE and FLAWS T1 values (B) appears to be mostly due to the resolution difference between the scans, as highlighted by the white arrows. Top left arrow: negative difference (B) between the MP2RAGE (A) and FLAWS (C) T1 maps due to the presence of GM/CSF partial volume voxels in the FLAWS T1 map. Top right arrow: positive difference (B) between the MP2RAGE (A) and FLAWS (C) T1 maps due to the increased number of CSF voxels in the MP2RAGE T1 map. Bottom left arrow: positive difference (B) between the MP2RAGE (A) and FLAWS (C) T1 maps due to the increased partial volume effect between the basal ganglia structures and surrounding WM in the MP2RAGE scan

FIGURE S8 B_1^+ map overlaid on FLAWS2 to show that low B_1^+ values were found in the inferior brain regions and near the hear canals (A) and frontal sinuses (B)

FIGURE S9 Sagittal slices of a FLAWS T1 map without post-hoc correction (A,B). The corresponding slices of the B_1^+ map are also shown (C,D). The blue ROI (A,C) delineates the WM segmentation for B_1^+ values above 100% of the nominal flip angle. The green ROI (B,D) delineates the cortical GM segmentation for B_1^+ values above 100% of the nominal flip angle. The white arrows design segmentation error (here, inclusion of CSF voxels in the WM and cortical GM segmentations). A qualitative assessment suggested that the WM and cortical GM T1 measurements remains stable for B_1^+ values above 100% of the nominal flip angle, thus, indicating that the T1 mapping divergence found for high B_1^+ in Figure 5 is likely due to segmentation errors (highlighted by the white arrows here)

How to cite this article: Beaumont J, Gambarota G, Saint-Jalmes H, et al. High-resolution multi- T_1 -weighted contrast and T_1 mapping with low B_1^+ sensitivity using the fluid and white matter suppression (FLAWS) sequence at 7T. *Magn Reson Med*. 2021;85:1364–1378. <https://doi.org/10.1002/mrm.28517>